Research Article

Ahmed Salah Abood, Mohammed Y. Fattah* and Ageel Al-Adili

Experimental investigation of dynamic soil properties for modeling energy-absorbing layers

https://doi.org/10.1515/eng-2022-0557 received September 13, 2023; accepted November 09, 2023

Abstract: Modeling the propagation of waves in geomechanics is an essential part of dynamic analysis. In geotechnics, the study of the interaction between the soil and the foundation is particularly interesting. In order to mimic low-speed operating types (less than 1,500 rpm), this study details the creation of a dependable and efficient approach for designing and fabricating the steel box container. When employed as a boundary, an absorbing layer drastically reduces the amount of wave reflection that occurs inside the limited region. The present effort is split into two halves. The first step is to calculate the damping layer's damping constants, subgrade response modulus, damping ratio, shear modulus, vibration amplitude, and resonant frequency. The second section focuses on the dynamic study of the circular foundation by measuring the vibration amplitude, acceleration, velocity, and displacement caused by harmonic vibration machines. The findings demonstrate that simple material borders prevent the wave from dissipating as a consequence of reflection. Attenuation of waves is possible when the absorbing layer of energy represents semi-infinite soil. When absorbing just one layer, the vertical displacements at positions located at the box side boundary and its base decreased by 65, 63, and 67%, respectively. However, it dropped by 97, 96, and 98%, respectively, when two absorbent layers were used. On the basis of these promising results, the model results were compared with and without the absorbing layer. It would appear that the modeling of the absorbing layer, which is designed as two layers, has been satisfied for low speeds of harmonic vibration.

Keywords: absorbing energy, dynamic load, investigation, soil structure

e-mail: 40011@uotechnology.edu.ig

Ahmed Salah Abood: Civil Engineering Department, University of Technology, Baghdad, Iraq

Ageel Al-Adili: Civil Engineering Department, University of Technology,

Baghdad, Iraq, e-mail: 40077@uotechnology.edu.iq

1 Introduction

When evaluating the condition of moisture-sensitive soils, geotechnical engineers have to do the following things: figure out sizes and motions, figure out what causes changes in volume, figure out what causes baseline discomfort, come up with alternative foundation designs and mitigation strategies, and figure out which soils are sensitive to moisture [1].

The dynamic forces of the machinery are transferred to the soil through the foundation, which is the essential notion underlying the construction of the foundation. In other words, the energy of the dynamic forces is transmitted to the ground through the foundation. The ground absorbs energy that is traveling in all directions. If the earth under the foundation is multilayered instead of solid, then some energy from the bottom layer must be reflected to the top layer and then to the system as a whole. The flow of energy from the ground up to the earth is shown in a standard diagram in Figure 1 [2].

The combined pressure from the machine block and the ground's foundation during the static state is what causes tumor deformations. When the machine is subjected to dynamic forces, the forces are transmitted to the ground through the base. Activating the dynamic interaction between the foundation and the soil modifies the dynamic responsiveness of the machine's foundation system. In contrast to the frame foundation type, the influence is quite significant for the kind of foundation. It is possible that more than one layer beneath the base influences the energy transfer mechanism. This is accomplished via the interaction of three distinct wave types: primary or pressure waves (P-wave), secondary or shear waves (Swave), and surface or Rayleigh waves (R-wave). R-waves, in comparison with S-waves and P-waves, carry a much more significant fraction of the input energy (by a factor of 60 or more). The automated basis is, therefore, more heavily influenced by the R-wave [2].

Figure 2a depicts the dynamic loading pattern that occurs as a consequence of using a reciprocating or revolving machine. Figure 2(b) demonstrates that this dynamic

^{*} Corresponding author: Mohammed Y. Fattah, Civil Engineering Department, University of Technology, Baghdad, Iraq,

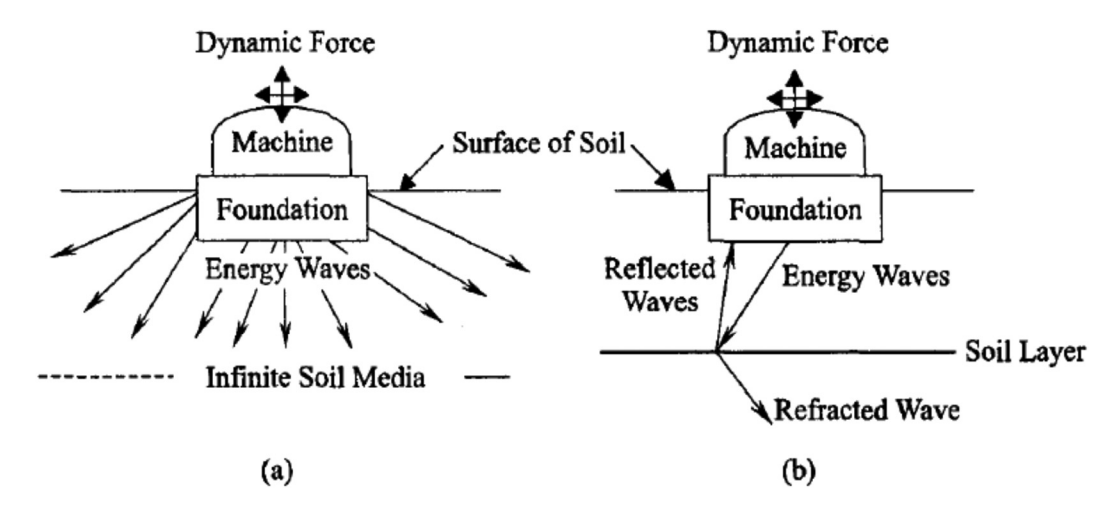


Figure 1: A typical example of energy dissipation from a building's base to its surrounding soils [2]. (a) Soil as single layer and (b) soil as layered media.

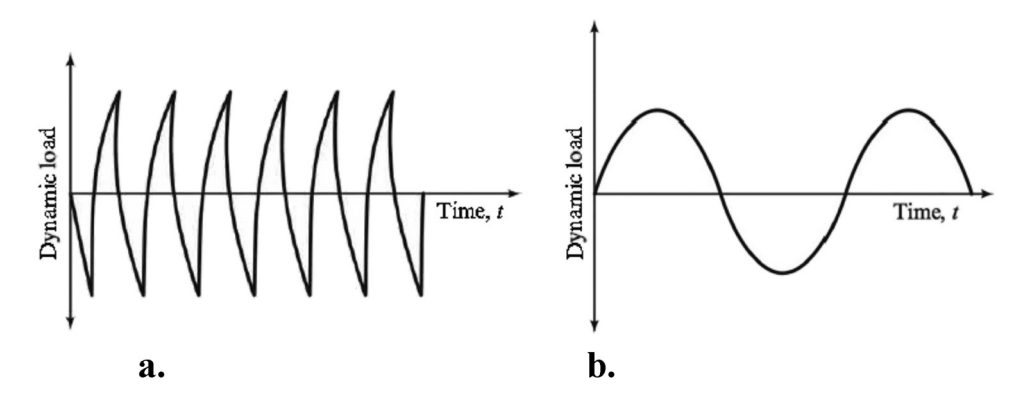


Figure 2: (a) Normal load with time for a slowly rotating machine and (b) a sinusoidal simplification [3].

load's slightly sinusoidal character may allow it to approach perfection. Figure 3a depicts the single-pulse tension produced in the soil when the hammer impacts the base. The workload typically rises with time, reaches its highest point in the future ($t_1 = t$), and then falls back down to zero. Figure 3b depicts the loading pattern (vertical acceleration) produced by pile

hammering. The dynamic loading from an earthquake can never be predicted. Pregnancy outcomes are very uncertain and shift dramatically over time in a random pregnancy, according to research by Das and Luo [3].

There is a rising need for a safety system that allows people to work safely alongside machinery robots or

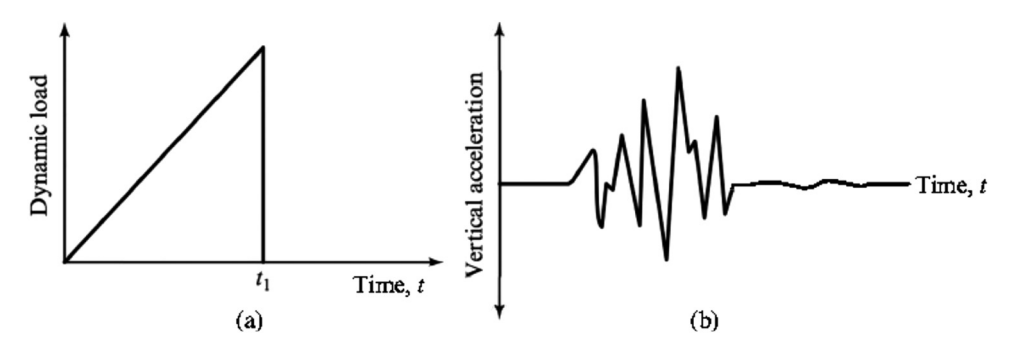


Figure 3: Loading diagrams have been constructed to account for the vertical component of ground acceleration brought on by driving piles as well as the transitory loading from a single hammer stroke. (a) Transient load; (b) Displacement [3].

dynamic machinery. Because dynamic machines or machinery robots are strong, harmful accidents and crashes must be avoided by maintaining an appropriate distance between the moving machine and the operator [4].

Saturated clay was employed in Al-Wakeel et al.'s [5] presentation of a solution for typical unbounded domains, in which the unbounded domain may be replaced by a thin energy absorption layer thanks to the domain's properties.

Sadighi and Salami [6] concluded that under the lowvelocity impact, the mechanical behavior of elastomeric and crushable foams is examined experimentally and numerically. The thickness and strain rate sensitivity impacts on the low-velocity impact response were investigated in detail. The potential of developing dynamic variables for three different types of materials was also examined, which does not demonstrate significant strain rate dependency. It has been demonstrated that increasing the thickness of specimens has no significant effect on the impact characteristics. As a result, dynamic parameters may be defined to forecast impact qualities based on static features for different thicknesses of specimens.

There are two major distinctions between the dynamic structure system and the dynamic soil-structure interaction system. In the first place, there is an unlimited characteristic. Werkle and Volarevic [7] analysis takes into account both the effect of radiation on the damping model, which gives a more realistic boundary condition, and the interaction of the structure with the foundation, which gives a more realistic boundary shape.

Fattah et al. [8] used the software Mod-MIXDYN to investigate how well transmission boundaries perform in dynamic analyses of soil-structure interactions. Transmission barriers were found to eliminate reflections in all three of the studied boundary circumstances (fixed borders, infinite boundaries, and viscous boundaries). With viscous borders and mapped infinite elements, this conclusion holds true as well.

Abdulrasool et al. [9] suggested a dependable and efficient method for the numerical simulation of an unbounded domain (the semi-infinite extension). When employed as a boundary, an absorbing layer drastically reduces the amount of wave reflection that occurs inside the limited region. The damping constants (β_s and α_d), elasticity module (*E*), subgrade response module (K), and natural frequency of the soils (ω_n) are only a few of the parameters of the absorbing layer that need to be evaluated. Also included is a finite element (FE) study of the strip foundation's dynamics performed in Open-Sees 2D. The soil was assumed to be linearly elastic, and the foundation is subjected to harmonious stimulation. According to the findings, wave attenuation occurs when an unbounded region of soil is represented by an energy-absorbing layer. Furthermore, the numerical model has shown that the existence of the absorbent layer would cause a decrease in the maximum amplitude of displacement [10].

The influence of material damping on the dynamic impedance functions of a circular disk embedded in homogeneous elastic half-space was analyzed by Sasmal and Pradhan [11] using one-dimensional wave propagation in cones (cone model), and the results were presented in the form of dimensionless plots to observe the more realistic response of machine foundations. Three different types of material damping models, viz., the spring and damping coefficients of the embedded foundation are then computed in a wide range of frequency of excitation under vertical and horizontal modes of vibration varying the influencing parameters, namely, dimensionless frequency (a_0) , Poisson's ratio (v), embedment ratio (e/r_0) , and damping ratio (ξ). The outcomes from the present analysis suggested that the spring coefficient is nonlinearly affected by the dimensionless frequency and embedment ratio for both modes of vibration. The effect of material damping on the spring coefficient is only significant for $a_0 > 2$, irrespective of the damping model used.

Surapreddi and Ghosh [12] investigated the influence of shape on the system and vibration transmission characteristics of block machine foundations under dynamic loading. A series of block vibration tests were conducted on model foundations laid on the local soil available at IIT Kanpur, India, to evaluate the system characteristics of machine foundations. The vibration transmission characteristics of the foundations were investigated using a 3D FE analysis. It was observed that the shape of foundations significantly influences the system characteristics. The circular and square foundations perform better than the rectangular foundations at higher loads. In contrast, the vibration transmission characteristics of block foundations are unaffected by the shape of the foundations.

Ajel et al. [13] used active barriers to experiment with vibration isolation by open and in-filled trenches. Filled with (rubber with native cohesive soil) mixes ranging from 20 to 40% rubber content, it produced screening rates ranging from 3 to 58% approximately. High rubber content and frequency are connected with better screening. Furthermore, when combined with the original cohesive soil to make a trench-filling material, the locally available tire chips proved inexpensive and efficient in vibration isolation.

Awchat et al. [14] stated that there is a separation gap between different codes, which can be compared to determine the minimum separation required to prevent pounding between the structures. The maximum lateral displacement on the roof and the time period of the adjacent buildings were compared with and without SSI. There is a significant increase in lateral displacement, separation distance, and time period considering SSI. It was found that the Indian code overestimates the separation distance.

Gypseous soils have been studied in the past within the classical framework of soil mechanics that is related to saturated condition. As such, they are characterized as collapsible, problematic soils that suffer large settlement and have significant loss of strength under long-term flooding. Little studies dealt with dynamic response of machine foundations on gypseous soil.

The objective of this study is to demonstrate the wave propagation as a result of reflection when the border of elementary material is applied. First, the dynamic properties of gypseous soils were determined. It is required to validate that when the energy's layer of absorption resembles a semi-infinite layer of soil, wave attenuation could be visible. The change of the vertical displacements when utilizing two absorbent layers is to be investigated.

2 Manufacturing of a model dynamic machine foundation

A small-scale (1:10) model was created to replicate a physical model of the machine foundation and to investigate energy loss and damping in saturated and unsaturated soils of varying degrees of saturation under a dynamic load of the harmonic form at various frequencies and load amplitudes. Calibration processes have been performed on each component of the gadget, and measuring sensors have also been integrated. The majority of the experiments were conducted at University of Technology Laboratory in Civil Engineering Department.

Three steel boxes containing all the system's gadgets, attachments, and sensors were produced for the research. Before being employed, the data loggers, sensors, and other devices used in the study were calibrated using a series of experimental procedures, to create a steel container box that resists and dampens low waves and frequencies produced by the harmonic vibration machine.

2.1 Manufacturing of steel boxes with an absorbing layer

The box is separated into two major components based on the desired operation frequency, as follows:

2.1.1 Steel container box

The specifications of the model container box are 500 mm in length, 500 mm in width, and 570 mm in height, with a steel plate thickness of 6 mm. The box has an aperture at the bottom with a high-pressure valve to manage the entry of water needed to saturate the soil model, as well as a water-level gauge (clear pipe, 46 mm size, and 10 bar capacity) to monitor the water level within the soil model. Screws and steel nuts with rubber washers were used to attach all sections of the model and the motor system to reduce and increase the absorption of vibration frequencies produced by the harmonic vibration engine.

The steel foundation's tensile test was performed in accordance with the required standard American society for testing and materials (ASTM) E8M [15]. This was carried out in order to determine the steel plate's elasticity modulus since it was utilized for the box and foundation. Table 1 displays the findings of the steel plate's material characteristics. Additionally, to guarantee accurate measurement, all of the components of the motor system and steel box model were made using laser cutting technology. The steel container box is shown in Figure 4.

2.1.2 Absorbing layer of box

To absorb and dampen the frequency waves created by the machine system, two layers of absorbent material (10 mm thick per layer) were applied to the inside surfaces of the iron box. Each absorbent layer is made up of two materials (rubber and polystyrene). This model dimension was used to replicate low-speed operation for dynamic testing (less than 1,500 rotations per minute). Figure 5 depicts a fabricated steel container box with an absorbent coating.

Forced vibration experiments with counterrotating weights were performed to determine the factors influencing absorption-layer characteristics. According to Chopra [16], equations (1) and (2) are used to compute damping constants (α_d and β_s) for individual elements in the energy absorption layer:

Table 1: Steel plate that has mechanical characteristics for the manufacturing of container boxes and foundations

Test type	Magnitude
Unit weight (y _t), kN/m ³	77.5
Modulus of elasticity (<i>E</i>), kN/m ²	363,220
Poisson's ratio (v)	0.285

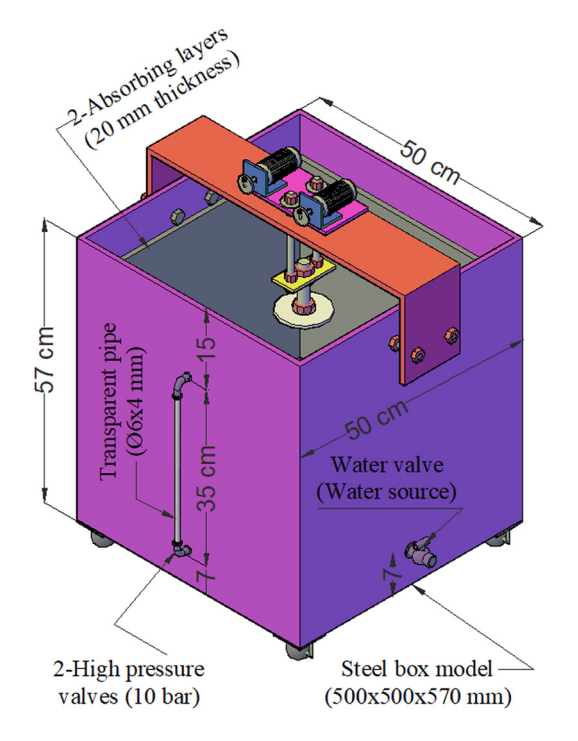


Figure 4: Steel container box.



Figure 5: Steel container box with constructed absorbent layers.

$$c = [(m \cdot \alpha_{\rm d}) + (k \cdot \beta_{\rm s})], \tag{1}$$

$$\frac{1}{2} \begin{bmatrix} \frac{1}{\omega_{n1}} & \omega_{n1} \\ \frac{1}{\omega_{n2}} & \omega_{n2} \end{bmatrix} \begin{bmatrix} \alpha_{d} \\ \beta_{s} \end{bmatrix} = \begin{bmatrix} D_{z1} \\ D_{z2} \end{bmatrix}, \tag{2}$$

where c is the average of damping coefficient (N s/m), β_s is the damping constant (Beta), α_d is the damping constant

(alpha), m is the mass of machinery and foundation (kg), k is the spring constant (N/m), ω_n is the natural frequency of circular (rad/s), and D_z is the damping ratio.

This work used two frequencies (12 and 15 Hz) to determine A_z , B_z , D_z , c_z , k_z , $\omega_{\rm n}$, $f_{\rm n}$, $f_{\rm m}$, and shear modulus (G), as given by Das and Ramana [17]. The damping constants ($a_{\rm d}$ and $\beta_{\rm s}$) were then determined by solving equations (1) and (2) for the natural frequencies. The $f_{\rm m}/f_{\rm n}$ ratio is then calculated using equation (15); the value must be more than one, and the bigger the value, the greater the damping rate; however, this will come at the sacrifice of money and time, as well as being dependent on the nature and significance of the research or project case. The absorbing-layer parameters are provided in Table 3.

$$D_z = \frac{c_z}{c_{cz}} = \frac{0.425}{\sqrt{B_z}},\tag{3}$$

$$B_{z} = \left[\left(\frac{1 - \mu}{4} \right) \times \left(\frac{m}{\rho r_{0}^{3}} \right) \right] = \left[\left(\frac{1 - \mu}{4} \right) \times \left(\frac{W}{\gamma r_{0}^{3}} \right) \right], \tag{4}$$

$$m = \frac{W}{g},\tag{5}$$

$$c_z = \frac{(3.4r_0)}{(1-\mu)} \sqrt{G\rho},$$
 (6)

$$c_{cz} = 2\omega_{\rm n} m = 2\sqrt{k_{\rm z} m}, \qquad (7)$$

$$G = \frac{k_z(1 - \mu)}{4r_0},\tag{8}$$

$$k_z = \left(\frac{4Gr_0}{1-\mu}\right) = m \cdot \omega^2 = \frac{P}{u},\tag{9}$$

$$\omega = \omega_{\rm n} = 2\pi f_n = \sqrt{\frac{k_z}{m}} = \sqrt{\frac{g}{u}}, \tag{10}$$

$$f_{\rm n} = \frac{1}{2\pi} \sqrt{\frac{k_{\rm z}}{m}},\tag{11}$$

$$f_{\rm m} = \frac{f_{\rm n}}{\sqrt{(1 - 2D_{\rm z}^2)}},$$
 (12)

$$A_{\rm z} = \left(\frac{2m_{\rm e}e_{\rm o}}{m}\right) \times \left(\frac{B_{\rm z}}{0.85\sqrt{B_{\rm z} - 0.18}}\right),$$
 (13)

$$O(t) = m\ddot{u} + c_7 \dot{u} + k_7 u, \tag{14}$$

$$\frac{f_{\text{resonance}}}{f_{\text{operating}}} = \frac{f_{\text{m}}}{f_{\text{n}}} > 1.0, \tag{15}$$

where B_z is the modified mass ratio; c_{cz} is the coefficient of critical damping (N s/m); W is the total machinery and foundation masses (kN); ρ and γ represent soil density in

6 — Ahmed Salah Abood et al. DE GRUYTER

kg/m³ and kN/m³, respectively; g is the ground acceleration (g = 9.81 m/s²); μ is the Poisson's ratio; r_o is the radius of the circular foundation (m); G is the dynamic shear modulus of the soil (kPa); f_n is the frequency of natural circular (Hz); f_m is the resonant frequency (Hz); A_z is the amplitude vibration at frequency resonance (mm); and m_e is the mass of eccentricity (kg); e_o is the distance of eccentricity (mm), P is the Maximum of vertical load (N); Q(t) is the total force (N); u is the amplitude displacement (mm), u is the amplitude velocity (m/s), and u is the amplitude acceleration (m/s²).

2.2 Soil properties

The soil used in this study was granular soil. Taken from a depth (0.6–2.5 m) approximately below the natural ground level, the groundwater level was not observed. To determine the physical parameters of the soil, a routine battery of tests was conducted. Table 2 provides an illustration of the specifics of the soil's physical characteristics. The Unified Soil Classification System (USCS) classifies the soil as silty sand "SM" as demonstrated by Abood et al. [18].

Table 2: Physical and chemical characteristics of the soil [18]

Character	istic	Magnitude	Reference
Specific gravity	G _s	2.43	ASTM [19]
Water content	<i>w</i> _c , %	1.59	ASTM [20]
Atterberg limits	liquid limit, %	20	ASTM [21]
	plastic limit, %	16	
	plasticity	4.0	
	index, %		
Particle size	Gravel	1.0	ASTM [22]
distribution by wet	(>4.75 mm)		
sieving (%)	Sand	79	
	(4.75-0.075)		
	Fines	20	
	(<0.075 mm)		
D ₁₀ (mm)	D ₁₀	0.0053	
D ₃₀ (mm)	D ₃₀	0.13	
D ₆₀ (mm)	D ₆₀	0.28	
Coefficient of	C_{u}	52.8	_
uniformity			
Coefficient of	C_{c}	11.4	_
curvature			
Classification of soil	USCS	SM	ASTM [23]
Maximum dry density	$ ho_{\sf d\ max}$	1.71	ASTM [24]
(g/cm ³)	e_{min}	0.42	
Minimum dry density	$ ho_{\sf d\ min}$	1.20	ASTM [25]
(g/cm ³)	e_{max}	1.03	
Total sulfate content	(SO_3)	21.07%	BS 1377 [26]
Gypsum content	(χ')	44.7%	BS 1377 [26]
(CaSO ₄)			

Table 3: Absorbing layer's characteristics

Property	Operating frequency (f_n)		
	900 cpm (15 Hz)	720 cpm (12 Hz)	
Dry soil density (ρ_d), gm/cm ³	1.34	1.34	
Net eccentricity mass ($m_{\rm e}$), g	28.0	28.0	
Masses of machinery and foundation (m), q	3,585	3,585	
Natural circular frequency (ω_n), rad/s	94.2	75.4	
Spring constant (k_z) , kN/m	31.812	20.381	
Poisson's ratio, (μ)	0.33	0.33	
Radius of foundation (r_0) , mm	50	50	
Dynamic shear modulus (G), kPa	10,657	68,276	
Damping coefficient (c_z), N s/m	95.9	76.8	
Coefficient of critical damping	675.4	540.6	
(c_{cz}) , N s/m			
Damping ratio (D_z)	0.14196	0.14197	
Resonant frequency (f _m), Hz	15.31	12.25	
Max. displacement (<i>u</i>), mm	1.106	1.726	
Alpha (α_d)	11.9		
Beta (β_s)	0.00167		
Average of damping coefficient		42.7	
(c), N s/m		2.50	
Modified mass ratio (B_z)	3.50		
Amplitude of vibration (A_z), mm f_m/f_n	1.02	0.971 1.02	

2.3 Logging software and a harmonic vibration machine

A box steel model was built to perform dynamic tests on saturated and unsaturated soils at different low-speed waves with other factors such as relative density, saturation degree, shape and depth of foundation, and operating frequencies in order to assess the viability of the idea in a controlled laboratory setting, as performed by Abdulrasool et al. [27].

2.3.1 Vibration machine

To test the notion in a laboratory setting, a small-scale oscillator was developed. A 2-mass oscillator is another name for this sort of equipment. The associated equipment required for producing vibration consists of two alternating current motors that work together but rotate in opposite directions. Each motor has a power rating of 350–400 W, a voltage range of 12–24 V, and an alternating current motor speed controller with a range of 0.1–3,000 rpm. The speed of the motor and the oscillator may be modified by altering the voltage given to the motor via

the speed control unit, which is set from 5 to 40 Hz depending on the cyclic frequency required. The speed of the motor and oscillator may be changed using the speed regulator panel, as demonstrated by Fattah et al. [28] and Abdulrasool et al. [27].

To measure the frequency of the system, a mechanical component is attached to the oscillator's disk and hooked up to a tachometer. One eccentric weight (m_e = 44.8 g) was used in accordance with the search criteria and was placed on a spinning disk with a diameter of 70 mm and a thickness of 6 mm. This weight is situated at an eccentricity distance of 27.5 mm from the rotation axis (e_o). The similar eccentric weight component on the opposite motor is abandoned by the horizontal component of force, and vice versa. The vertical component of the force is the only one that persists [16]. The harmonic vibration excitation device is depicted in Figure 6.

The German Research Society for Soil Mechanics adopted this equipment, which is featured in numerous textbooks, including Parakash [29] and Das and Ramana [17]. The amplitude of harmonic vibrating force (Q_0) at vertical places may be computed as follows:

$$Q_0 = 2m_{\rm e}e_0\omega,\tag{16}$$

where e_0 is the eccentricity distance (m), m_e is the eccentricity mass (kg), ω is the circular frequency of rotating masses (rad/s), and Q_0 is the amplitude vibrating force (kN).

The mechanical oscillator generates a sinusoidal harmonic vibration; the vertical vibrating force Q(t) at all times may be characterized as follows:

$$Q(t) = Q_0 \sin(\omega t), \tag{17}$$

where t is the total time (s) and Q(t) is the amplitude vibrating force at all time (kN).

2.3.2 Accelerometer sensor

The accelerometer can detect the dynamic acceleration caused by motion or a sudden shock, as well as the static acceleration caused by gravity, with varied ranges and resolutions. It may be used to speed up any application. The measuring range of accelerometer sensors is ±16g. Sensors used in saturated and unsaturated soil were waterproofed with a polyurethane coating and coated with a plastic casing, which was then filled with silicone and hammered with screws to allow the sensor to attach to the soil. The displacement, acceleration, and dynamic velocity values with time for each axis and at the sites where the sensor is positioned within or surrounding the model were determined using the data acquired by the acceleration sensor and its data logger. Figure 7 shows the shape and properties of the accelerometer sensor.

2.3.3 Data logger

FastDAQ is a versatile data recorder that may be used in routine laboratory testing. It is a device for storing monitoring parameters that is precise, rapid, and accurate.

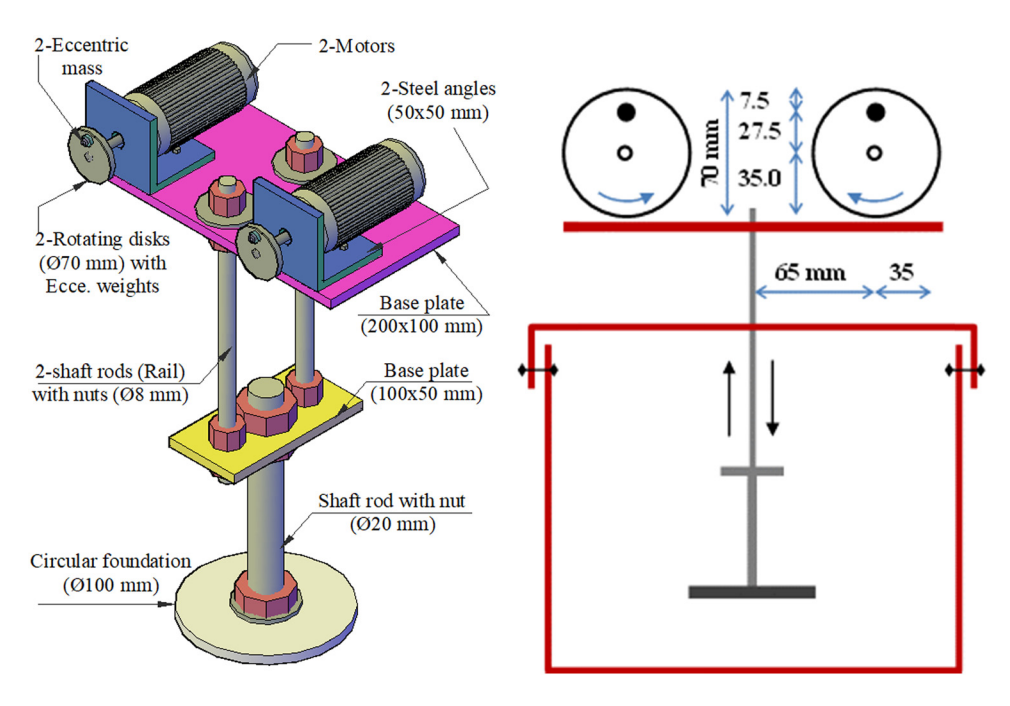


Figure 6: Vibration machine excited by harmonic load.

8 — Ahmed Salah Abood *et al.* DE GRUYTER



Figure 7: Accelerometer sensor.

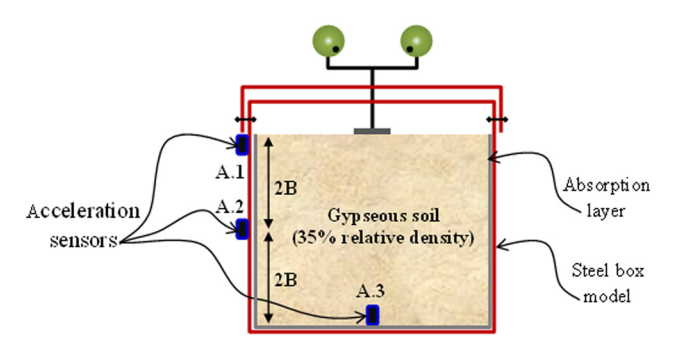


Figure 8: Accelerometer sensors distributed on the box model to detect the damping rate of the absorption layer.

FastDAQ is used to retrieve data from one-dimensional consolidation, total stress, pore water pressure, deformation, accelerometers, and load cells. FastDAQ is simple to integrate into a test or monitoring system and can collect data in minutes. FastDAQ is ideal in this sense since it allows for quick and easy data acquisition, eliminating compliance issues. It can also range from one to numerous channels, with each channel receiving a different sort of sensor depending on the study. In this study, a single device with four channels (Model: FastDAQ V.1.01_4Ch) and accelerometer sensors was employed.

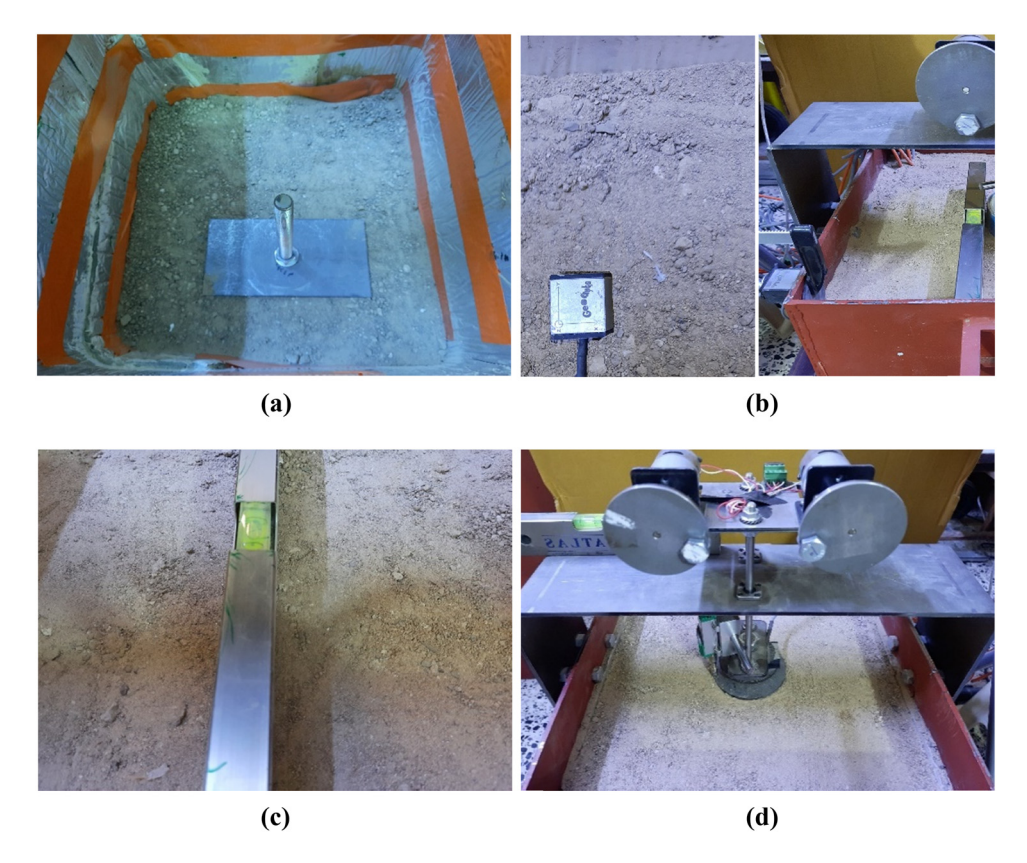


Figure 9: A rundown of the model preparation stages: (a) compaction of soil at 5 cm layer, (b) placing sensor in a model, (c) checking by a bubble level, and (d) placing of foundation at a center.

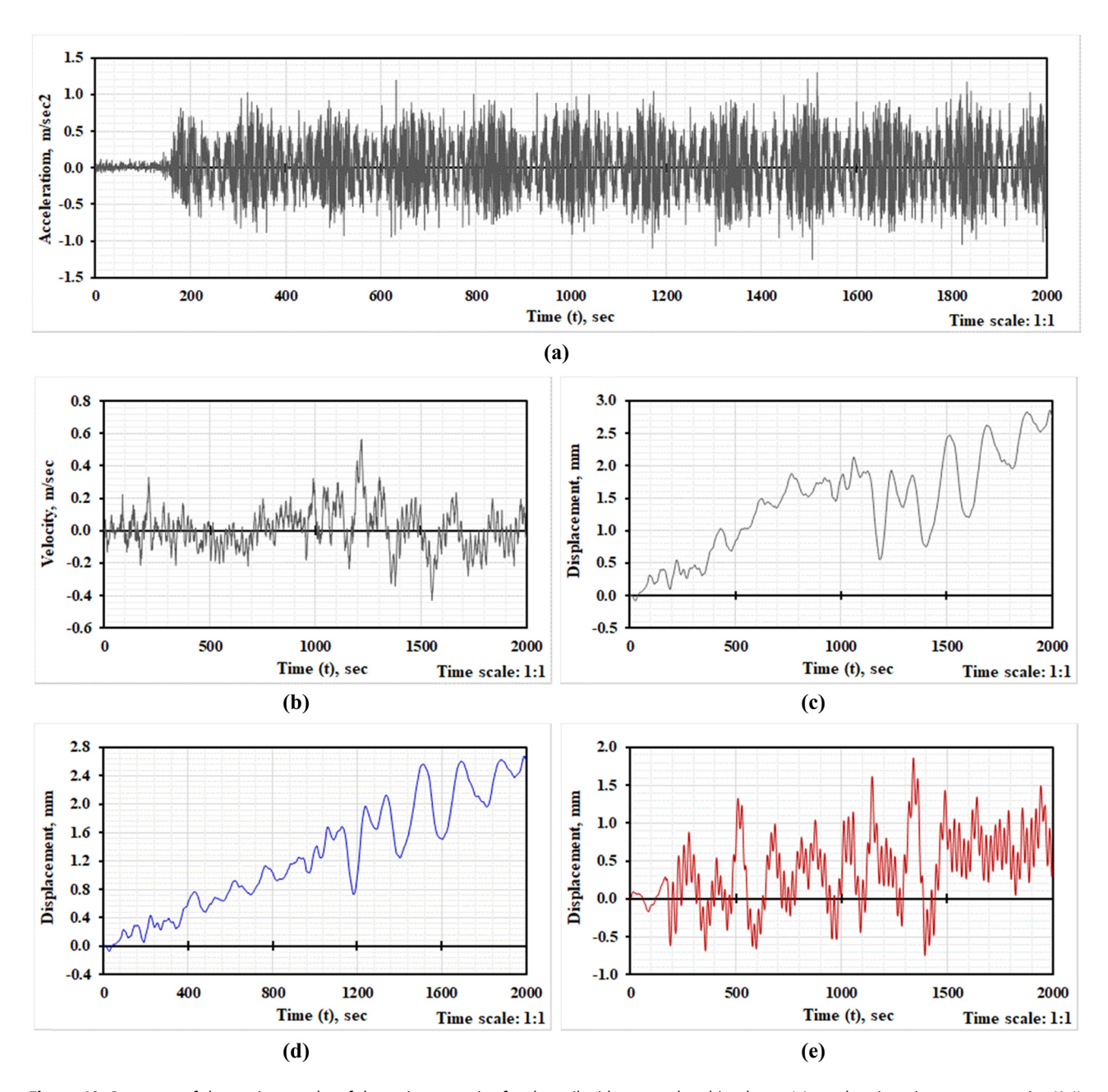


Figure 10: Summary of the testing results of dynamic properties for the soil without an absorbing layer: (a) acceleration–time curve at point (A.1) without any absorbing layer, (b) velocity–time curve at point (A.1), (c) displacement–time curve at point (A.1), (d) velocity–time curve at point (A.2), and (e) displacement–time curve at point (A.3).

2.4 Model preparation

- a. To guarantee a homogenous density for the whole model, the soil sample is produced in layers (50 mm per layer) and then placed within the box and levelled with careful hand compaction using an appropriate steel or wooden tool.
- b. Considering the location of accelerometer sensors inside the model in accordance with the exact places and levels depicted in Figure 8.
- c. Following dirt compaction and installation in the steel box, the surface was levelled and examined with a bubble level.
- d. The harmonic vibration system foundation model was put in the center of the box.

An overview of the model preparation stages is presented in Figure 9.

For dynamic tests, a box model with the dimensions (500 \times 500 \times 570) mm was utilized to represent low-speed

10 — Ahmed Salah Abood et al. DE GRUYTER

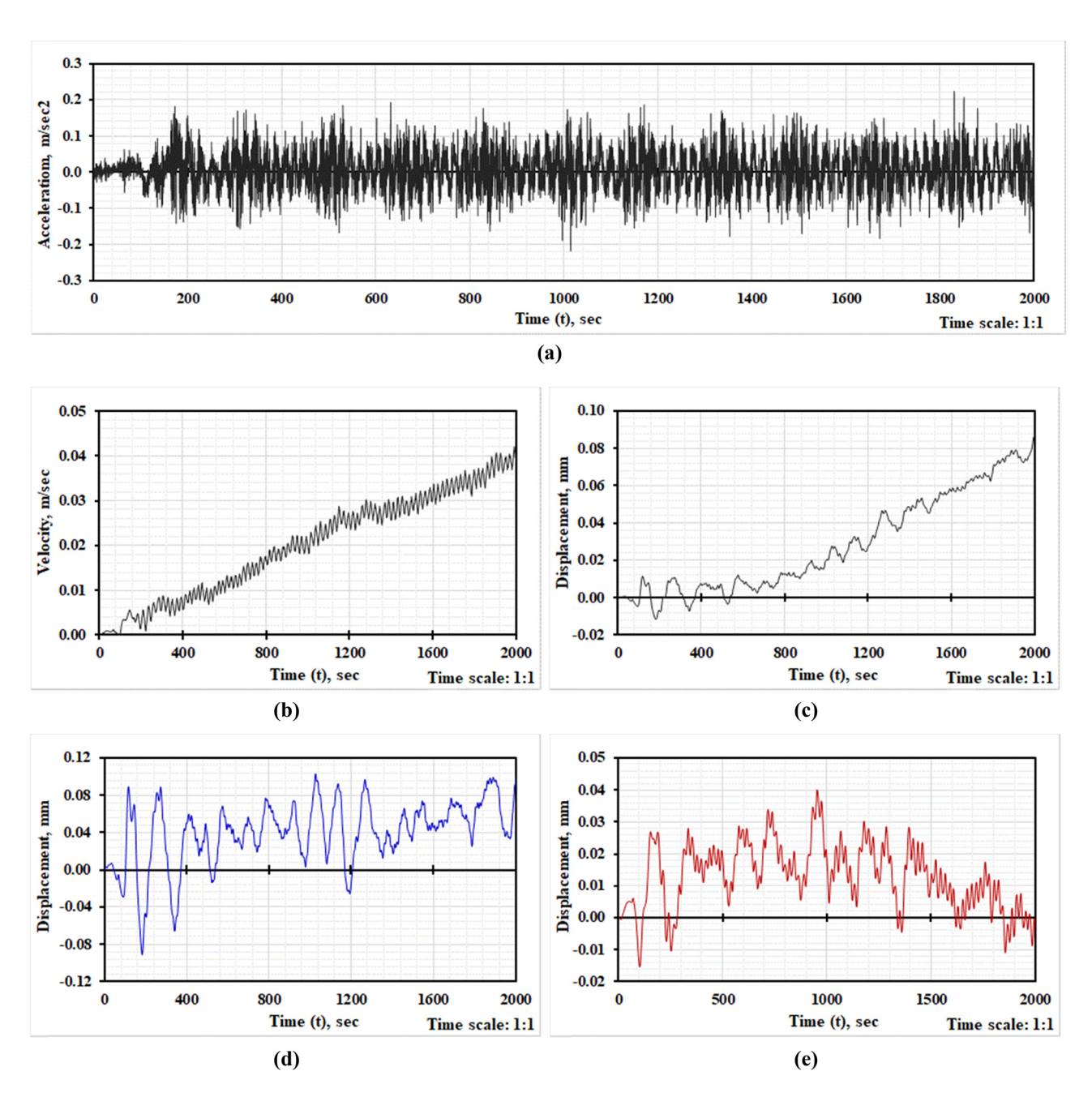


Figure 11: Summary of testing results for dynamic properties of the soil with two absorbing layers: (a) acceleration—time curve at point (A.1) with two absorbing layers, (b) velocity—time curve at point (A.1), (c) displacement—time curve at point (A.1), (d) velocity—time curve at point (A.2), and (e) displacement—time curve at point (A.3).

operating types (less than 1,500 rpm or less than 25.0 Hz). A soil sample with a relative density of 35% was placed inside the box and the dry density of the soil in the model was 1.23 g/cm³. The acceleration sensor was attached to the exterior. In order to determine the frequencies and the ratio of the connection to the outside of the box when the absorption layer is absent and the damping ratio when it is present, a variable frequency load of 720 and 900 cyclic/min was then applied on a circular basis with a diameter of 100 mm, as shown in Figure 8.

3 Presentation and discussion results

Table 3 summarizes the characteristics of the absorbing soil layer as calculated by the previous equations.

Figures 10 and 11 demonstrate the typical dynamic property results for the soil without and with two absorbing layers, respectively. Table 4 also shows a summary of vertical

Table 4: Summary of vertical displacement findings at various positions in the model while employing the absorber layer

Amplitude displacement (u_z), mm	15.0 Hz frequency (f _n)		
	Without any absorbing layer	With absorbing a layer	With absorbing 2 layers
Point (A.1)	2.812	0.982	0.084
Point (A.2)	2.671	0.988	0.107
Point (A.3)	1.956	0.645	0.039

displacement findings at various positions in the models when the absorber layer is used. Because its application minimizes horizontal displacement, the absorbing layer has a considerable influence on horizontal displacement. The displacement response of the foundation is minimized when the infinite domain is used as opposed to the elementary bounds. Based on these promising findings, a comparison of the model with and without the absorbent layer in the border was performed. The absorbing layer modeling, which was designed to mimic radiation conditions at infinite boundaries, looks to have been completed.

The amplitudes of displacement or velocity or acceleration of the machine foundation should be within permissible limits. The permissible limits are depending upon the operating frequency of the machine as well as soil type and characteristics. In no case should the permissible amplitude exceed the limiting amplitude prescribed for the machine by the manufacturer [30]. All machines under normal operation usually induce a periodic dynamic load on the foundation. This induced dynamic load causes some portion of the soil underlying the foundation to be subjected to vibration, and it is essential that the natural frequency of this vibration should be far away from the operating frequency of the machine [31].

The findings demonstrate that the wave does not fade as a result of reflection when the border of elementary material is applied. When the energy's layer of absorption resembles a semi-infinite layer of dirt, wave attenuation could be visible. One layer of absorption at sites A.1, A.2, and A.3 decreased the vertical displacements by 65, 63, and 67%, respectively. However, it decreased by 97, 96, and 98% at the same points when utilizing two absorbent layers.

A comparison between the model with and without the absorbent layer produced these positive findings. It appears that the harmonic vibration's low speed has been taken into account in the modeling of the absorbent layer, which is constructed as two layers.

4 Conclusions

- 1. Based on the natural frequency and eccentric mass of unsaturated and saturated soils in terms of amplitude of acceleration, velocity, and displacement, a new steel box model with an absorbing layer for low-speed harmonic vibration machines was proposed in this study.
- 2. The constructed box model's findings for dynamic loading using typical equations and relationships have been effectively confirmed with those of experimental testing.
- 3. A comparison between the model with and without the absorbent layer is made in light of these encouraging results. It appears that the two-layer modeling of the absorbent layer has been satisfied for low harmonic vibration rates.
- 4. When absorbing just one layer, the vertical displacements at positions located at the box side boundary and its base decreased by 65, 63, and 67%, respectively. However, it dropped by 97, 96, and 98%, respectively, when two absorbent layers were used.

For future studies, it is suggested studying the foundations of the machine under different types of gypseous soils by measuring the shear waves that travel within the model and evaluating the damping rate on the soil samples at different densities and saturation degrees.

Funding information: The author states no funding involved.

Conflict of interest: The authors state no conflict of interest.

Data availability statement: Most datasets generated and analyzed in this study are comprised in this submitted manuscript. The other datasets are available on a reasonable request from the corresponding author with the attached information.

References

- Houston WN, Houston SL. Infiltration studies for unsaturated soils. [1] In: Alonso EE, Delage P, editors. Unsaturated SoilsProc. 1st Int. Conf. on Unsat. Soils, Paris. Balkema, Rotterdam: Presses des Ponts et Chaussees; 1995. p. 869-75.
- Bhatia KG. Foundations for industrial machines handbook for [2] practising engineers. D-CAD, Rohini, New Delhi; 2008.
- Das BM, Luo Z. Principles of soil dynamics. 3rd edn. USA: Cengage [3] Learning; 2017.
- Malm T, Salmi T, Marstio I, Montonen J. Dynamic safety system for collaboration of operators and industrial robots. Open Eng. 2019;9(1):61-71. doi: 10.1515/eng-2019-0011.

- [5] Al-Wakeel SF, Fattah MY, Karim HH. Dynamic analysis of foundations on saturated clay using an energy absorbing layer. Eng Tech J. 2011;29(11):2189–2201.
- [6] Sadighi M, Salami S. An investigation on low-velocity impact response of elastomeric & crushable foams. Open Eng. 2012;2(4):627–37. doi: 10.2478/s13531-012-0026-0.
- [7] Werkle H, Volarevic J. Modeling of Dynamic soil-structure-interaction in the three-dimensional finite element analysis of buildings. 2nd European Conference on Earthquake Engineering and Seismology, Istanbul, Turkey; 2014. p. 1–12.
- [8] Fattah MY, Hamood MJ, Dawood SH. Dynamic response of a lined tunnel with transmitting boundaries. Techno-Press J Earthq Struct. 2015;8(1):275–304. doi: 10.12989/eas.2015.8.1.275.
- [9] Abdulrasool AS, Fattah MY, Salim NM. Application of energy absorbing layer to soil-structure interaction analysis. IOP Conference Series: Materials Science and Engineering. Vol. 737; 2020. p. 0120971–10. doi: 10.1088/1757-899X/737/1/012097.
- [10] Fattah MY, Ahmed BA, Ali AF. Experimental investigation on the damping characteristics in dry and saturated sands. Mech Based Des Struct Mach Int J. 2022. doi: 10.1080/15397734.2022.2104310.
- [11] Sasmal SK, Pradhan PK. Effect of material damping on the impedance functions of an embedded circular foundation under vertical and horizontal excitation. Innov Infrastruct Solut. 2021;6(4). doi: 10. 1007/s41062-020-00370-3.
- [12] Surapreddi S, Ghosh P. Impact of footing shape on dynamic properties and vibration transmission characteristics of machine foundations. Int J Geosynth Ground Eng. 2022;8:2. doi: 10.1007/ s40891-021-00347-x.
- [13] Ajel HA, Al-Jubair HS, Ali JK. An experimental study on vibration isolation by open and in-filled trenches. Open Eng. 2022;12(1):555–69. doi: 10.1515/eng-2022-0011.
- [14] Awchat GD, Monde A, Sirsikar R, Dingane R, Dhanjode G. Seismic pounding response of neighboring structure using various codes with soil-structure interaction effects: focus on separation gap. Civ Eng J. 2022;8(2):308–18. doi: 10.28991/CEJ-2022-08-02-09.
- [15] ASTM E8M. Standard test methods for tension testing of metallic materials. American Concrete Institute; 2004.
- [16] Chopra AK. Dynamics of structures: theory and applications to earthquake engineering. Englewood Cliffs, New Jersey: Prentice-Hall. Inc: 2012.
- [17] Das BM, Ramana GV. Principles of soil dynamics. 2nd edn. Stamford: Cengage Learning Publishers; 2011.

- [18] Abood AS, Fattah MY, Al-Adili AS. Studying characteristics and strength of the unsaturated gypseous soil with various saturation degrees. Eng Technol J. 2023;41(11):1309–24. doi: 10.30684/etj. 2023.140119.1453.
- [19] ASTM D 854-00: Standard test method for specific gravity of soil solids by pycnometer. American Society for Testing and Materials 2017
- [20] ASTM D 2216-00: Standard test method for laboratory determination of water (Moisture) content of soil and rock by mass. American Society for Testing and Materials. 2017
- [21] ASTM D 4318-00, Standard test methods for liquid limit, plastic limit, and plasticity index of soils. American Society for Testing and Materials. 2017
- [22] ASTM D 422-00: Standard test method for particle size-analysis of soils. American Society for Testing and Materials. 2017
- [23] ASTM D 2487-00: Standard practice for classification of soils for engineering purposes (Unified Soil Classification System). American Society for Testing and Materials. 2017
- [24] ASTM D 4253-00: Standard test method for maximum index density and unit weight of soils using a vibratory table. American Society for Testing and Materials. 2017
- [25] ASTM D 4254-00: Standard test method for minimum index density and unit weight of soils and calculation of relative density. American Society for Testing and Materials. 2017
- [26] British Standard Institution. Method of testing soils for civil engineering purposes. B.S; 1990. p. 1377.
- [27] Abdulrasool AS, Fattah MY, Salim NM. Displacements and stresses induced by vibrations of machine foundation on clay soil of different degrees of saturation. Case Stud Constr Mater J. 2022;17:e013271–15. doi: 10.1016/j.cscm.2022. e01327.
- [28] Fattah MY, Al-Mosawi MJ, Al-Ameri AFI. Stresses and pore water pressure induced by machine foundation on saturated sand. Ocean Eng. 2017;146:268–81. doi: 10.1016/j.oceaneng.2017.09.055.
- [29] Parakash S. Soil dynamics. New York, USA: McGraw-Hill; 1981.
- [30] Chen S, Chen L, Zhang J. Dynamic response of a flexible plate on saturated soil layer. Soil Dyn Earthq Eng. 2006;26(6):637–47.
- [31] Fattah MY, Al-Mosawi MJ, Al-Ameri AF. Dynamic response of saturated soil - foundation system acted upon by vibration. J Earthq Eng. 2017;21(7):1158–88. doi: 10.1080/13632469.2016. 1210060.